

EMI REDUCTION ON HIGH-SPEED PCB USING ELECTROMAGNETIC
BANDGAP STRUCTURE

MUSAAB ABDULGHANI QASEM

A thesis submitted in
fulfillment of the requirement for the award of the
Master's Degree of Electrical Engineering

Faculty of Electrical and Electronic Engineering

Universiti Tun Hussein Onn Malaysia

NOVEMBER 2016

DEDICATION

For my beloved mother and father, I send my sincere appreciation and love for your continuous support and Doa'a during the period of my studies. For my brothers and sisters, your constant encouragement are indeed a great motivation for me. I would also like to extend my gratitude towards my supervisor, Dr. Zuhairiah binti Zainal Abidin and Co-Supervisor Prof. Mohd Zarar Mohd Jenu.

I hope that the proposed designs and thesis will be beneficial for researchers working with microwaves, photonics, and its applications.

ACKNOWLEDGEMENT

I would like to express my sincere appreciation to my supervisor, Dr. Zuhairiah binti Zainal Abidin and Co-supervisor Prof. Mohd Zarar Mohd Jenu for the support given throughout the duration of completing this thesis.

The cooperation given by the UTHM EMC center is also highly appreciated. Appreciation also goes to everyone involved directly or indirectly towards the compilation of this thesis. Last but not least, many thanks is given to my beloved friends and family members, Mom, and Dad.

ABSTRACT

The need for high-speed printed circuit board design whilst maintaining signal integrity and EMC standards have increased over the years in the modern integrated circuitry field. The use of electromagnetic bandgap structures (EBGs) have been demonstrated to provide excellent reduction of electromagnetic interference (EMI). In this study, a three by three planar of spiral, with and without patch were designed, simulated and fabricated on a low-cost FR4 substrate with permittivity of 4.3 and thickness of 1.6 mm. The designs of spiral EBGs with and without patch have the dimensions of 36 mm x 36 mm covering 9 unit cells. The performance of the designed EBGs were simulated and measured experimentally, and it was found to be in acceptable agreement. It was found that the spiral EBG without patch experienced a bandgap that covers from 4.5 to 6.3 GHz by using a dispersion diagram. Conversely, the bandgap for the spiral EBG with patch structure was found to be from 4.5 to 7.8 GHz with wider bandwidth. Owing to the desirable results demonstrated by the spiral EBG design with patch, it was then integrated into the high-speed circuit design to suppress the EMI emitted by the board. In this work, two low and three high-speed PCB designs were fabricated to track the desired EMI levels above 4.5 GHz. The third design of the high-speed PCB emitted the highest radiation emission (4.54 GHz) was selected for integration. The spiral EBG with patch structure successfully suppressed the EMI that occur at 4.54 GHz. Its effectiveness further suggests that the proposed EBG spiral with patch structure design is appropriate for EMI suppression that may occur from 4.5 to 7.8 GHz.

CONTENTS

DECLARATION	i
DEDICATION	ii
ACKNOWLEDGEMENT	iii
ABSTRACT	iv
CONTENTS	v
LIST OF TABLES	viii
LIST OF FIGURES	ix
LIST OF SYMBOLS AND ABBREVIATIONS	xii
LIST OF APPENDIXES	xiii
LIST OF PUBLICATIONS	xiv
CHAPTER 1 INTRODUCTION	1
1.1 Research Background	1
1.2 Problem Statement	2
1.3 Research Objective	3
1.4 Research Scope	3
1.5 Research Contribution	4
1.6 Thesis Outline	4
CHAPTER 2 THEORY AND LITERATURE REVIEW	6
2.1 Introduction	6
2.2 Electromagnetic Bandgap Structure	7
2.3 Electromagnetic Bandgap (EBG) Classification	8
2.4 EBG Characterizations	10
2.4.1 Dispersion Diagram	10
2.4.2 In-phase Reflection	11
2.4.3 Scattering Parameter	15

2.5 Spiral EBG Structure Characteristics	17
2.6 An Overview of EBG Application for EMI Suppression on PCBs	19
2.6.1 EBG Structure for SSN Suppression	19
2.6.2 EBG Structures on Parallel-Plate	21
2.6.3 EBG Structure on Optical Transceiver	21
2.6.4 Split-Ring Resonators on High-Speed Circuits	22
2.7 Summary	24
CHAPTER 3 METHODOLOGY	25
3.1 Design of EBG Structure	27
3.1.1 Analytical Study	27
3.1.2 Mathematical Model	27
3.1.3 Mathematical Calculations	30
3.2 The Design of Spiral EBG with Patch	34
3.4 EBG Characterization	35
3.4.1 Dispersion Diagram Model	35
3.4.2 Suspended Microstripline Method	38
3.5 Designs of High Radiated Emission PCB	39
3.5.1 Low-speed PCB Designs	39
3.5.1.1 Single-Sided Design	39
3.5.1.2 Double-Sided Assembly	41
3.5.2 High-Speed PCB, (HSPCB) Designs	43
3.6 Spiral EBG with Patch and HSPCB Integration	49
3.7 Experimental Set Up in Semi-Anechoic Chamber (SAC)	50
CHAPTER 4 RESULT AND DISCUSSION	52
4.1 Spiral EBG without Patch Design	52
4.1.1 Equivalent Circuit of Spiral without Patch Structure	52
4.1.2 Dispersion Diagram	53
4.1.3 Simulated and Measured Transmission Coefficient, S_{21} for Spiral EBG without Patch Planar	54
4.2 Spiral EBG with Patch Design	55
4.2.1 Dispersion Diagram	55

4.2.2 Simulated and Measured Transmission Coefficient, S_{21} for Spiral EBG with Patch	56
4.3 Comparison of Transmission Coefficient, S_{21} of Spiral EBG With and Without Patch Planars	57
4.4 Radiated Emission, RE	59
4.4.1 Low-Speed PCB	59
4.4.2 High Speed PCB	62
4.4.2.1 First Design of HSPCB	63
4.4.2.2 Second Design of HSPCB	64
4.4.2.3 Third Design of HSPCB	65
4.5 Integration of Third Design and Spiral EBG with Patch Planar	66
4.6 Summary	67
CHAPTER 5 CONCLUSION AND FUTURE RECOMMENDATION	68
5.1 Conclusion	68
5.2 EBG Characterization	68
5.3 PCB Design and RE Test	69
5.3.1 Low Speed PCB	69
5.3.2 High Speed PCB	70
5.4 EBG Structure Integration into HSPCB	70
5.5 Recommendations for Future Work	71
REFERENCES	71
APPENDIX A	73
APPENDIX B	78

LIST OF TABLES

2.1: Turns effect on f_c and BW reduction (Moghadasi, et al, 2008)	18
3.2: Geometrical parameters of spiral with and without patch unit cell	35
3.3: Geometrical parameters of spiral shrinkable design	40
3.4: Single sided PCB design features	40
3.5: Double sided PCB design features	41
3.6: First design of HSPCB features	44
3.7: Second design of HSPCB features	45
3.8: Third design of HSPCB features	74

LIST OF FIGURES

Figure 2.1: EBG functioning concept	7
Figure 2.2: Example of 1-D EBG design (Kim et al., 2000)	8
Figure 2.3: Mushroom-like EBG Array (Sievenpiper et al., 1999).	9
Figure 2.4: A 3-D Slab EBG Structure (Ouassal et al., 2016)	9
Figure 2.5: (a) Simulated unit cell by dispersion diagram method (b) Dispersion diagram with different gap sizes G (Ouassal et al., 2016)	11
Figure 2.6: Waveguide model of in-phase reflection method	12
Figure 2.7: Unit cell dimensions	12
Figure 2.8: Waveguide model for unit cell simulations	13
Figure 2.9: Reflection Phase Diagram of an EBG unit cell	13
Figure 2.10: (a) Reflection phase of UC-EBG, (b) Frequency band vs. patch width (Yang & Rahmat-samii, 2003)	14
Figure 2.11: (a) Reflection phase of UC-EBG, (b) Frequency band vs. gap width (Yang & Rahmat-samii, 2003)	15
Figure 2.12: 3 by 3 EBG planar (a) Front view and (b) Back view (Alam, Islam, & Misran, 2012)	16
Figure 2.13: Transmission loss S_{21} of 3 by 3 EBG array with bridge width variation (Alam, Islam, & Misran, 2012).	16
Figure 2.14: Transmission loss S_{21} of 3 by 3 EBG array with bridge width variation (Alam, Islam, & Misran, 2012).	17
Figure 2.15: (a) Circular spiral EBG structure (b) Transmission coefficient S_{21} of circular EBG planar (Moghadasi et al., 2008)	18
Figure 2.16: (a) HIS EBG structure cascading board (b) Experiment set up of RE test. (c) Transmission coefficient, S_{21} comparison of PCB with/ without EBG structure.	21
Figure 2.17: (a) EBG structure on parallel plate. (b) Transmission coefficient S_{21} comparison of parallel plate with and without EBG structure.	21

Figure 2.18: (a) Optical transceiver. (b) EBG structure and experimental set up. (c) Measured S_{21} at 5 cm distance by monopole antenna (d) RE test readings.	22
Figure 2.19: (a) Complementary split-ring resonator PCB. (b) Transmission coefficient S_{21} comparison of CSRR and solid board.	23
Figure 3.1: Flowchart that illustrates the overall procedures of this research work	26
Figure 3.2: (a) Spiral EBG without patch unit cell (b) Sideview	30
Figure 3.3: Spiral EBG without patch equivalent circuit	32
Figure 3.4: Unit cell for spiral EBG without patch design	32
Figure 3.5: Equivalent circuit of spiral EBG without patch unit cell using ADS	33
Figure 3.6: Unit cell for spiral EBG with patch design	34
Figure 3.7: Brillouin zone definition on the spiral EBG structure	36
Figure 3.8: example of “dispersion diagram” of a 2D-periodic structure, based on Brillouin Zone definition (in this example the step of sweep is 30 degree) (Yang & Rahmat-samii, 2003).	36
Figure 3.9: Boundary conditions of spiral unit cell	37
Figure 3.10: Phase shift set up along the boundary conditions, CST (MWS)	37
Figure 3.11: (a) Top view of suspended microstrip line. (b) Bottom view of 3 by 3 spiral EBG without patch planar. (c) Side view	39
Figure 3.12: 3-D single-sided PCB	40
Figure 3.13: Top view of the single-sided layout.	41
Figure 3.14: Side view of double sided PCB	41
Figure 3.15: Top view of double-sided layout	42
Figure 3.16: First Design of HSPCB layout	45
Figure 3.17: Second design of HSPCB layout	46
Figure 3.18: Third design of HSPCB layout	48
Figure 3.19: Integration of 15 by 3 EBG planar and PCB layout	49
Figure 3.20: Semi-anechoic chamber, (SAC) system	50
Figure 3.21: PCB under test using semi-anechoic chamber, (SAC)	51
Figure 4.1: Frequency resonance from ADS for the spiral EBG without patch	53
Figure 4.2: Dispersion diagram of the spiral EBG without patch	54

Figure 4.3: Simulated and measured results for three by three spiral EBG without patch planar	55
Figure 4.4: Dispersion diagram of the spiral EBG without patch	56
Figure 4.6: Simulated and measured results for spiral EBG with patch planar	57
Figure 4.10: Comparison between measured results of spiral EBG with/without patch planar.	57
Figure 4.7: RE of Single sided low speed PCB	59
Figure 4.8: RE of Single sided low speed PCB	60
Figure 4.12: RE readings of double-sided design	61
Figure 4.10: RE readings of double-sided design	62
Figure 4.11: RE readings of first design of HSPCB	63
Figure 4.12: RE readings of second design of HSPCB	64
Figure 4.13: RE readings of third design of HSPCB	65
Figure 4.14: RE readings of third design HSPCB with spiral EBG with patch planar integration	66

LIST OF SYMBOLS AND ABBREVIATIONS

UTHM	-	University Tun Hussein Onn Malaysia.
EMC	-	Stands for Electromagnetic Compatibility
EMI	-	Stands for Electromagnetic Interference
RE	-	Stands for Radiated Emissions
EBG	-	Stands for Electromagnetic Bandgap
PCB	-	Stands for Printed Circuit Board
HSPCB	-	Stands for High-Speed Printed Circuit Board
W	-	Unit Cell metallic Width
L	-	Unit Cell metallic Length
W_{in}	-	Internal gap width with horizontal measuring
a	-	Internal gap width with vertical measuring
b	-	Upper half of Internal gap length with vertical measuring
c	-	Lower half of Internal gap length with vertical measuring
g	-	Gaps Width between sections
e	-	Length of Central Metallic Section
m	-	Metallic Width
d	-	Distance Between Middle Sections
G	-	Gap between Sections
t	-	Metallic Thickness
S	-	Section Width
P	-	Spiral Length
Z	-	Spiral Width
X	-	Internal gap Width
d	-	Dielectric Thickness

LIST OF APPENDICES

APPENDIX	TITLE
A	Mathematical Calculations
B	Matlab Code

LIST OF PUBLICATIONS

- Alshargabi, M. A., Abidin, Z. . Z., & Jenu, M. Z. M. (2015). High Speed PCB & Spiral with Patch EBG Planar Integration for EMI Reduction, (I4CT), 584–588.
- Alshargabi, M. A., Abidin, Z. Z., & Jenu, M. Z. . M. (2013). Spiral Electromagnetic Bandgap structure for EMI reduction. *RFM 2013 - 2013 IEEE International RF and Microwave Conference, Proceedings*, (1), 310–313.
- Alshargabi, M. A., Abidin, Z. Z., & Jenu, M. Z. . M. (2015). Novel Spiral With and Without Patch EBG Structures for EMI Reduction. *Jurnal Teknologi*.

CHAPTER 1

INTRODUCTION

1.1 Research Background

Controlling emissions and interferences have become a necessity in the design and manufacture of electronic devices for both civilian and military use. It is more cost effective to design a product with suppression designed into the printed circuit board (PCB) than to "build a better box." Containment measures are not always economically justified and may degrade as the electromagnetic compatibility (EMC) life cycle of the product is extended beyond the original design specification. For example, users usually remove covers from enclosures for ease of access during repair or upgrade. In many cases, sheet metal covers, particularly internal subassembly covers that act as partitioning shields are never replaced. The same goes for blank metal panels or faceplates on the front or rear of a system that contains a chassis or backplane assembly. Consequently, containment measures are compromised, and EMC with the end-use environment is affected. Proper layout of a PCB, with suppression techniques implemented, assists EMC compliance at the level of cables and interconnects, whereas box shielding (containment) does not.

Electrical engineers may focus on analog, digital, or system-level products but, regardless of their specialty, whatever they produce must be suitable for production. More often than not, the emphasis is placed on the functionality rather than on system integration. System integration is customarily assigned to product engineers, mechanical engineers, or others within an organization. Design engineers must now consider other aspects of the product design that includes the layout and production of PCBs that conforms to the EMC radiated emission tests such as CISPR 22 and CISPR 14-1. In

addition, the cost must be minimized during design, test, integration, and production. If a product fails to meet regulatory compliance tests (EMC and product safety), redesign or rework may be required.

1.2 Problem Statement

Electromagnetic radiation of high-speed circuits is considered as one of the most critical challenges to the electromagnetic interference (EMI), compatibility and reliability of electronic systems. The world of EMI and EMC design has undergone significant changes as the speed of processors, clocks, and digital communications links have increased. EMI is a complex mechanism that takes place at different levels including the chassis, board, component, and finally, the device level. There are many techniques of EMI suppressions to face this critical challenge such as shielding and filtering. Shielding is used to reduce the amount of electromagnetic radiation reaching a sensitive victim circuit. Shields are made of metal and work on the principle that electromagnetic fields are reflected and/or attenuated by a metal surface. Shielding can be a stand-alone solution, but it is more cost-effective compared to other suppression techniques such as grounding, filtering, and proper circuit-board design to minimize the loop area. Unfortunately, designers often leave shielding as a last option since the shields can be installed once the design is completed. Thus, this will increase the cost as the shielding will be customized to the actual radiating components on the printed board. If a metal enclosure is to be used, its shielding effect should be utilized. However, it is always better to reduce the noise inside the box than to rely on the shielding effectiveness (Texas Instrument,2010). Filters or decoupling capacitors are used to eliminate EMI and can be installed at either the source or the victim. It was investigated by (Montrose, 2011) that the magnitude of radiated electromagnetic interference (EMI) is significant based on physical placement of decoupling capacitors to digital components. The proposal of EBG structure for EMI suppression on high speed PCBs will overcome the drawback of using shielding or decoupling capacitors. This study employs new method that implemenent the integration of EBG structures into the PCB design to achieve EMI suppression with cost effective technique.

1.3 Research Objective

- (i) To design an EBG structure that operates within a frequency range of 4 to 8 GHz where existing methods have limitations for this frequency rang.
- (ii) To validate the simulation of the proposed EBG structure through experimental works.
- (iii) To design high source of radiated emission within frequency level of 4 to 8 GHz.
- (iv) To investigate the effectiveness of the EBG in reducing the EMI by integrating it into a bad high speed PCB design that produce high radiated emissions.

1.4 Research Scope

This work focused on the design, modeling and implementation of electromagnetic band gap (EBG) structures and high radiated emission source in the form of high speed printed circuit board. This work is devoted to design and model a planar EBG structure to be implemented for EMI suppression on high speed PCBs. The design of an EBG structure covers the frequency band within 4 to 8 GHz. At this frequency band of radiated emissions, the existing methods have not been costly effective such as shielding or are not efficient enough for high radiated noise. Therefore, the EBG structure will overcome this issue due to its unique behavior at such frequencies.

The research included three by three spiral EBG with and without patch array. Both designs have been simulated and measured using the commercially available software Computer Simulation Technology, CST and Advanced Design System, ADS. For measurements, the Agilent Vector Network Analyzer is used to validate the transmission coefficient (S_{21}) of the proposed spiral EBG designs.

This work also focused on the design of high source of radiated emissions at frequency band greater than 4 GHz. Thus, several designs have been implemented using SPICE tool which was proteus simulator and went under radiated emission test defined by CISPR22 regulations by using semi anechoic chamber, SAC at the Research Center of Applied Electromagnetics-Universiti Tun Hussein Onn Malaysia. Finally, the source of

high radiated emissions was selected according to the RE test readings and ready for integration stage. A new method of EMI suppression on noisy printed circuit board was developed and implemented by integrating spiral EBG with patch structure into the PCB board. Then, the developed integration went under radiated emission test for EMI detection.

1.5 Research Contribution

- (i) The integration of EBG structure into PCBs was introduced for the purpose of reducing the EMI levels.
- (ii) This research proposed spiral with and without patch EBG designs that have unique structure that exclude the existing of vias. This will make it practical to be integrated into many layers PCBs.
- (iii) One of the techniques that reduce EMI on PCBs is applying decoupling capacitors. At high frequencies, this technique is not sufficient. This research proposed the integration of EBG structure into high speed PCB and shows significant improve to EMI levels.

1.6 Thesis Outline

This thesis consists of five chapters. The chapters are briefly outlined as follows:

CHAPTER 1 explains the background, scope, research objectives and the problem statements of the project.

CHAPTER 2 discusses the theory of EBG design and past related works. This chapter explains the basic parameter of electromagnetic photonics, different types of EBG with distinct design concept. The methods of analysis for the simulation software as well as the measurements were also explained.

CHAPTER 3 describes the steps in designing two types of EBG structures and the integration of one type of the proposed EBG structures into the high-speed PCB design. The design begins with the mathematical representation of the lumped element model and followed by simulation, fabrication and finally the measurement.

CHAPTER 4 will present the results obtained from the study and followed by a discussion. The performances of all EBG structures and PCB designs that was simulated and verified experimentally.

CHAPTER 5 concludes the project with some suggestions for future design improvements on both the PCB and EBG structures.

CHAPTER 2

THEORY AND LITERATURE REVIEW

2.1 Introduction

Electromagnetic Interference (EMI) that affects electronic devices poses a critical challenge in the legalization of electronic equipment (Scogna, 2012). This challenge is further intensified by an increase in system integration motivated by the rise of clock functionality (Gagare & Kachare, 2014). EMI may be attributed to different hardware design stages including the device, the chip, the package, the printed circuit board, interconnects and components, the chassis, as well as the peripherals (Montrose, 2000). By means of either reducing radiated emission of the equipment or increasing their immunity to external interference, EMI could be reduced. Various strategies have been applied to mitigate such radiation emission unique to each of the aforementioned levels.

Electromagnetic noise or interference may be reduced but not limited to the isolation of critical components, shielding, matching, filtering, the addition of lossy materials and absorbers. Eliminating the source of EMI is clearly desirable, but does not necessarily translate or equate to a reduction in the susceptibility of the device to external sources. In a study conducted by (Iravani, 2007), lossy material and absorbers were applied to isolate interference between apertures or antennas sharing a common reference plane. Nonetheless, although lossy materials have desirable electromagnetic features, mechanical and thermal properties that can severely limit their applicability, the cost, on the other hand, can be an important factor as these materials need to be engineered to work with specific frequency bands.

Electromagnetic Bandgap (EBG) structures that have been proposed over the past few years possess inherent features that make them important in EMI/EMC applications (Yang, 2009). Previous works investigated the effectiveness of EBG structures in the suppression of unwanted electromagnetic energy in several applications. EBG structures are sufficient to reduce the coupling of antennas (Zarrabi, Mansouri, & Rahimi, 2014). Shahparnia & Ramahi (Shahparnia & Ramahi, 2007), on the other hand, used the EBG patches to suppress propagating waves within the power planes and parallel plates of printed circuit boards. Shahparnia et al. (Shahparnia, Member, Ramahi, & Member, 2004) also utilized EBG to suppress the radiation from Printed Circuit Boards (PCB), and they were used in for signal integrity purpose.

2.2 Electromagnetic Bandgap Structure

EBGs have attracted researchers due to their ability to control and manipulate the propagation of electromagnetic (EM) waves which produce forbidden frequency gaps in which propagation is prohibited and allow certain frequency to pass (Zarrabi, Mansouri, & Rahimi, 2014). At the forbidden band gap, all the electromagnetic wave will be reflected. Basically, the EBG can act as reflector for stop band gap. At other frequencies it will act as transparent medium. The EBG functioning concept of passing and reflecting the EM waves is illustrated in Figure 2.1

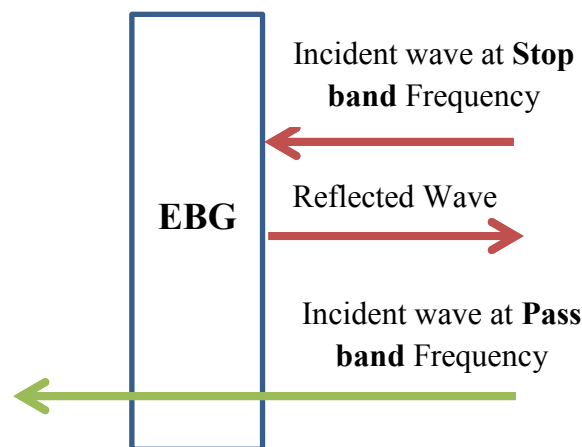


Figure 2.1: EBG functioning concept

EBG structures consist of periodic cells. Studies were conducted by (Alam, Islam, & Misran, 2012) (Aminian, Yang, & Rahmat-Samii, 2003) (Phuong, Chien, & Tuan, 2013) (Fei, Guo, Liu, & Wang, 2011) (Mohajer-iravani, Shahparnia, Ramahi, & Member, 2014), reported that the unique properties of electromagnetic bandgap (EBG) structures have made them applicable to many microwave applications. Two main interesting features associated with EBG structures are suppression of surface waves and in-phase reflection coefficient for plane waves (Aminian, Yang, & Rahmat-Samii, 2003). EBG structures can also be used in microstrip antenna design to enhance antenna performance by means of surface wave suppression (Majid et al., 2014). The EBG design can be implemented and optimized based on the substrate material, design geometrics, via involvements, lumped element model as will be explain in next subtopics.

2.3 Electromagnetic Bandgap (EBG) Classification

Electromagnetic band gap material is also known as type of metamaterials, which is realized by a periodic arrangement of dielectric materials and metallic conductors. According to their geometric configuration, they can be classified into three categories: (1) one-dimensional transmission line, (2) two dimensional planar surfaces, and (3) three-dimensional volumetric structures . Figure 2.2 shows an example of one-dimensional EBG transmission line design (Kim, Park, Ahn, & Lim, 2000).

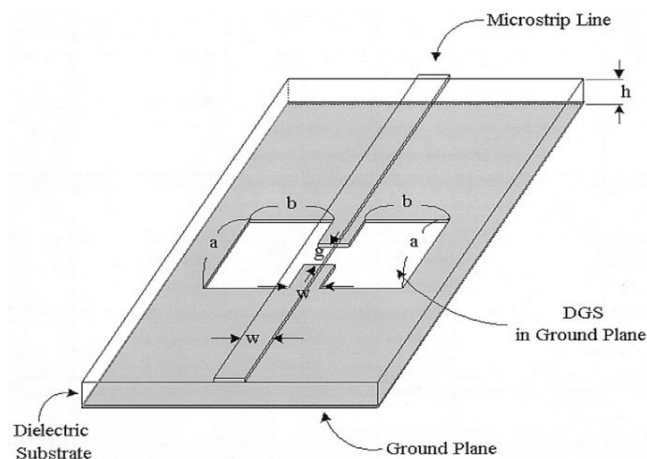


Figure 2.2: Example of 1-D EBG design (Kim et al., 2000)

Previous study of 2-D EBG structures by the name of mushroom-like EBG structure were proposed by (Sievenpiper, Zhang, Broas, & Yablonovitch, 1999). An example of a top view and side view of the Mushroom-like structure is illustrated in Figure 2.3.

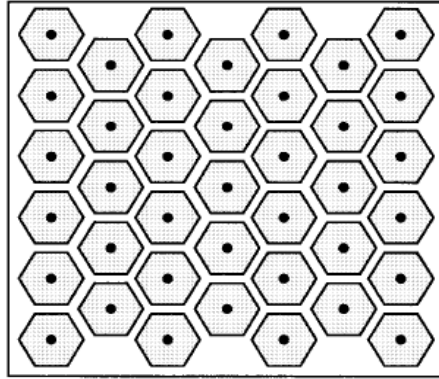


Figure 2.3: Mushroom-like EBG Array (Sievenpiper et al., 1999).

A study was conducted by (Ouassal, Shaker, Roy, & Chaharmir, 2016) shows an example of 3-D Multi-layer EBG structure that was comprised of 3-D Lattice of Square Rings as illustrated in Figure 2.4.

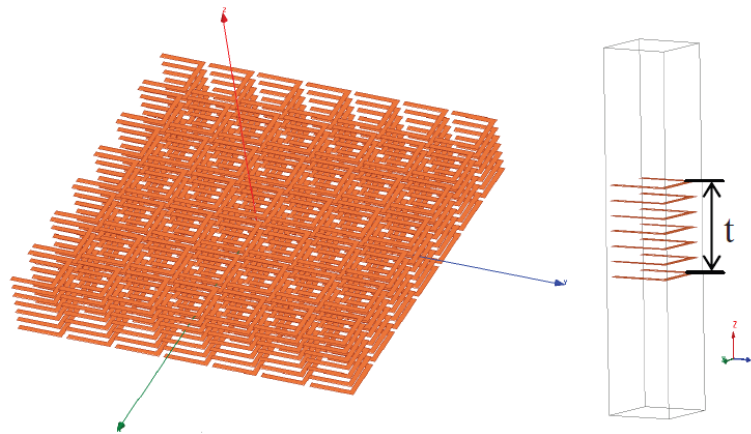


Figure 2.4: A 3-D Slab EBG Structure (Ouassal et al., 2016)

2.4 EBG Characterizations

There are several methods that were used commonly to investigate the frequency bandgap of EBG structures. The most common methods are the dispersion diagram, in-phase reflection, and scattering parameter as will be reviewed in the following subtopics.

2.4.1 Dispersion Diagram

For dispersion diagram method, the periodic boundary condition is considered on four sides of the unit cell. For the top of the unit cell a perfect matched layer (PML) boundary condition will be applied as an infinite periodic replication. The dispersion diagram has a vertical axis that shows the frequency and a horizontal axis that represents the values of the transverse wave number (k_x, k_y). The horizontal axis is defined by three remarkable points (Yang F., 2009):

$$\Gamma: \quad k_x = 0, \quad k_y = 0, \quad (2.1)$$

$$X: \quad k_x = 2\pi/(W + g), \quad k_y = 0, \quad (2.2)$$

$$M: \quad k_x = 2\pi/(W + g), \quad k_y = 2\pi/(W + g) \quad (2.3)$$

where;

Γ = reflection coefficient

X = surface reactance

M = wave factor

W = width of the EBG cell

g = gap of the EBG cell

As shown in Figure 2.5 (a), the EBG unit cell structure that was designed by (Ouassal et al., 2016). The dispersion diagram of the unit cell is illustrated in Figure 2.5 (b) where the variation of the parameter G has the effect on the bandgap as presented.

From the dispersion diagram, it is observed that the frequency band gap for the EBG unit cell shown in is between 5 GHz and 11 GHz considering $G = 0.1$ mm, which means that the surface wave inside this frequency band range will be suppressed.

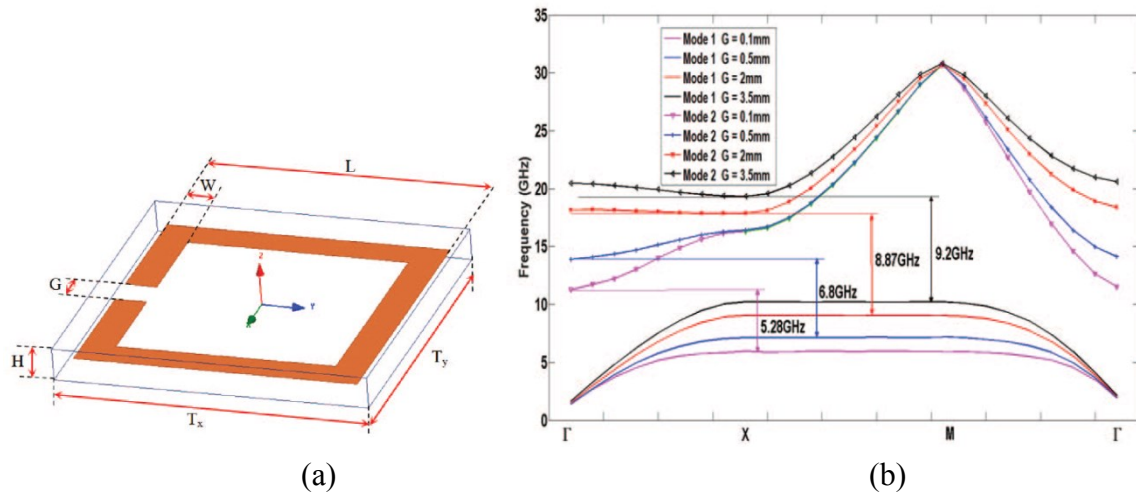


Figure 2.5: (a) Simulated unit cell by dispersion diagram method (b) Dispersion diagram with different gap sizes G (Ouassal et al., 2016)

2.4.2 In-phase Reflection

Reflection phase of EBG structures is very interesting topic where they exhibit unique response and behavior. In-phase reflection, the reflection property will be described. It can be defined as the ratio of the reflected waves over the incident waves at the destination surface.

The simulation model is realized by using an ideal TEM waveguide as illustrated in Figure 2.6. The periodic boundary conditions are assigned with perfect electric conductor, (PEC) in two parallel walls of the waveguide and with perfect magnetic conductor, (PMC) in the other two parallel walls. Thus, the adjacent walls offer perfect electric and perfect magnetic boundary conditions alternating circular around the longitudinal axis. The TEM wave is excited by a wave port travelling down the longitudinal axis of the waveguide.

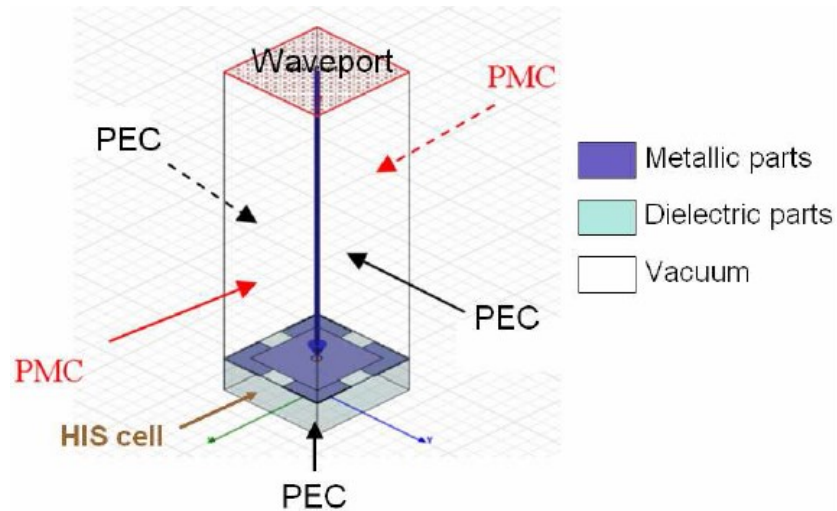


Figure 2.6: Waveguide model of in-phase reflection method

A study was conducted by (Islam & Alam, 2013) focuses on a compact uni-planar type EBG structure for a 2.4 GHz resonant frequency band is illustrated in Figure 2.7.

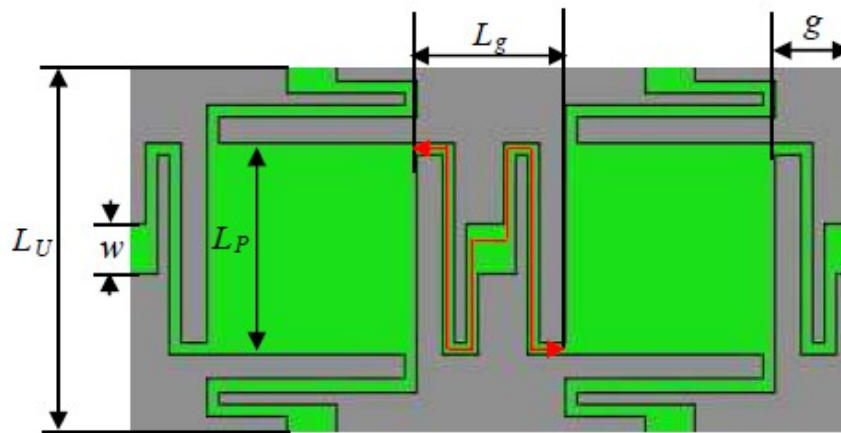


Figure 2.7: Unit cell dimensions

The reflection phase characteristic was examined with the simulated waveguide model as shown in Figure 2.8. The EBG unit cell was surrounded symmetrically by a pair of electric boundary and a pair of magnetic boundary planes whilst a wave port illuminated the surface from the top. The reflected phase from the EBG structure is normalized to the reflected phase from a PEC surface placed at the same height of EBG.

Figure 2.9 illustrates the reflection phase characteristic of the double-folded bend EBG structure. Reflection phase bandwidth is defined as the ratio of frequency bandwidth in which the reflection phase is between $90 \pm 45^\circ$ to the center frequency. The quadratic phase is necessary to obtain a good return loss (Yang & Rahmat-samii, 2003). The AMC point was located at 3.3 GHz, having a narrow bandwidth of 0.3 GHz (3.1 – 3.4 GHz). This method has the advantage of reduced time of simulations and ease.

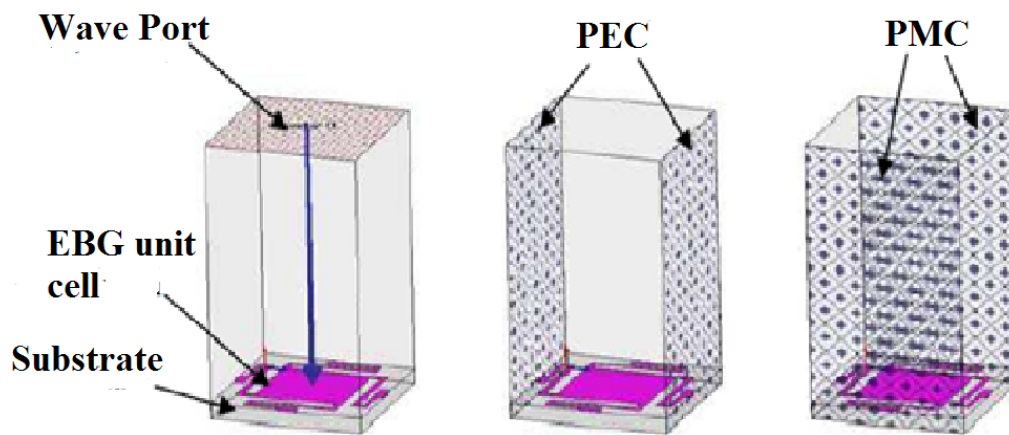


Figure 2.8: Waveguide model for unit cell simulations

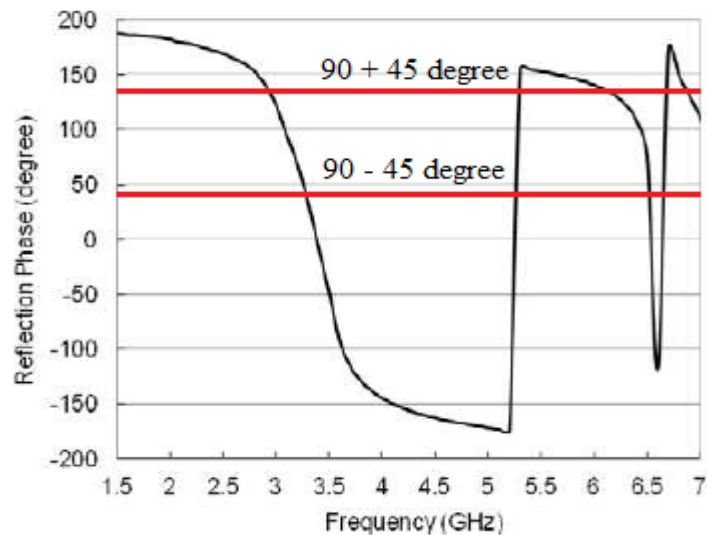


Figure 2.9: Reflection Phase Diagram of an EBG unit cell

The resonance frequency and the bandwidth of an EBG structure depends on the unit cell geometry together with substrate's relative dielectric permittivity and thickness (Phuong, Chien, & Tuan, 2013). Patch and metallic widths plays an important role in determining the frequency band (Yang & Rahmat-samii, 2003). The effect of the EBG metallic width, by keeping other parameters like the gap width, substrate permittivity, and substrate thickness the same is illustrated in Figure 2.10 (a) and (b).

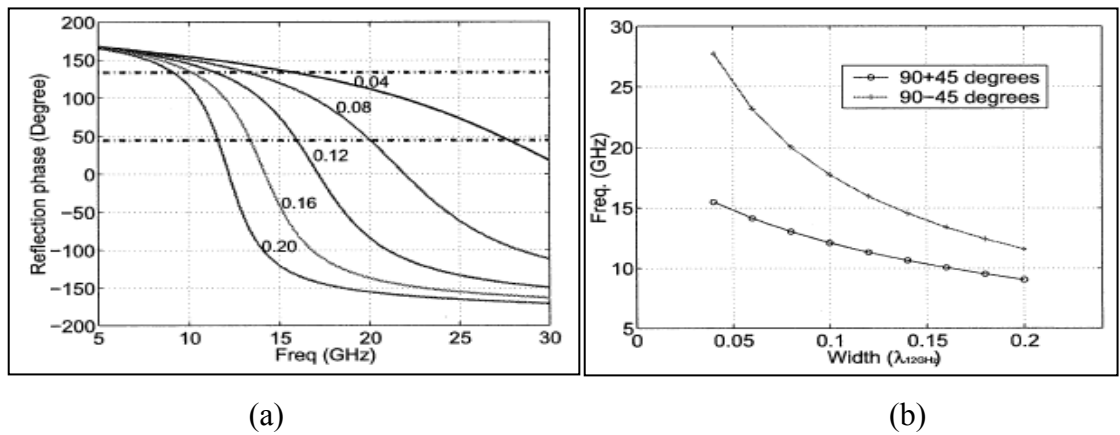


Figure 2.10: (a) Reflection phase of UC-EBG, (b) Frequency band vs. patch width (Yang & Rahmat-samii, 2003)

The distance between adjacent patches or metallic elements is known as the gap width. The variation of the gap width may also affect the frequency band of the EBG surface too as shown in Figure 2.11 (a) and (b).

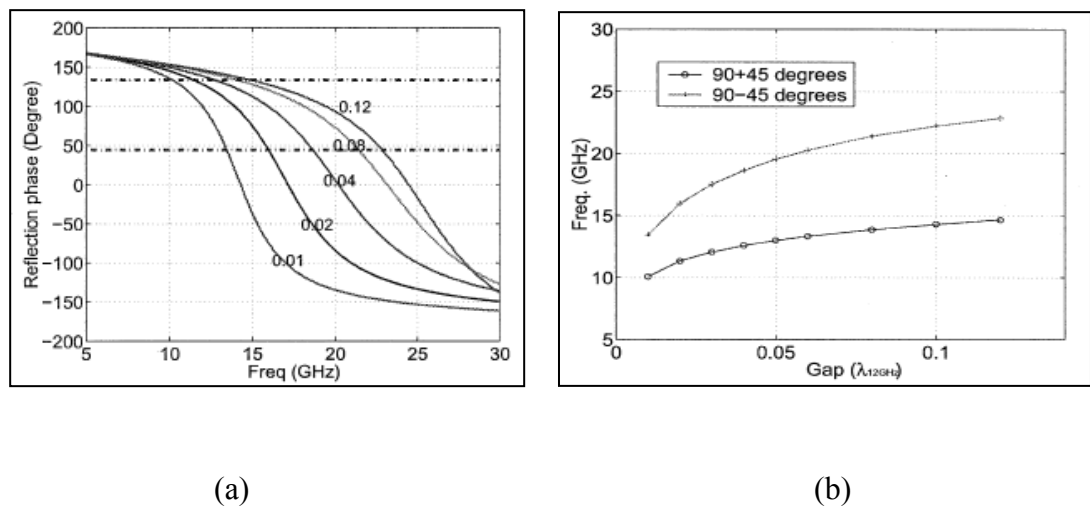
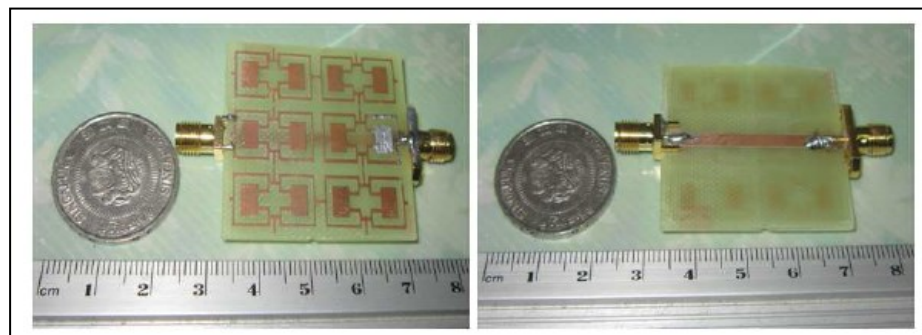


Figure 2.11: (a) Reflection phase of UC-EBG, (b) Frequency band vs. gap width (Yang & Rahmat-samii, 2003)

2.4.3 Scattering Parameter

In order to determine the transmission coefficient S_{21} of a finite structure considering the existing of a few periods, this method is used to find at which frequency the stop band is located. As the dispersion diagram assumes as an infinite structure without excitation, the scattering parameter method is much faster and somehow more realistic to what will be found in practice. Owing to use the strongly coupling structures, the characteristic of EBG is more obviously exhibited as compared to other techniques (Fan, Rong, Qing, Zhang, & Feng, 2003). This method is very similar to the implementation of an EBG as a filter.

The suspended microstrip line method is used to find the surface wave suppression characteristics of EBG structures. This method has been proven in achieving the desired characteristics as compared to the classical monopole method. Figure 2.12 (a) and (b) show a design of 3 by 3 EBG planar that was examined by suspended microstrip line method (Alam, Islam, & Misran, 2012). It can be clearly seen that changing the geometrical parameters such as metallic width or patch size, affect the EBG characteristics based on the concept of total inductance associated with the EBG geometry as shown in Figure 2.13 (Alam, Islam, & Misran, 2012). By considering the bridge width to be 1 mm, the stop band of the structure is from 4.5 to 10 GHz.



(a)

(b)

Figure 2.12: Three by three EBG planar (a) Front view and (b) Back view (Alam, Islam, & Misran, 2012)

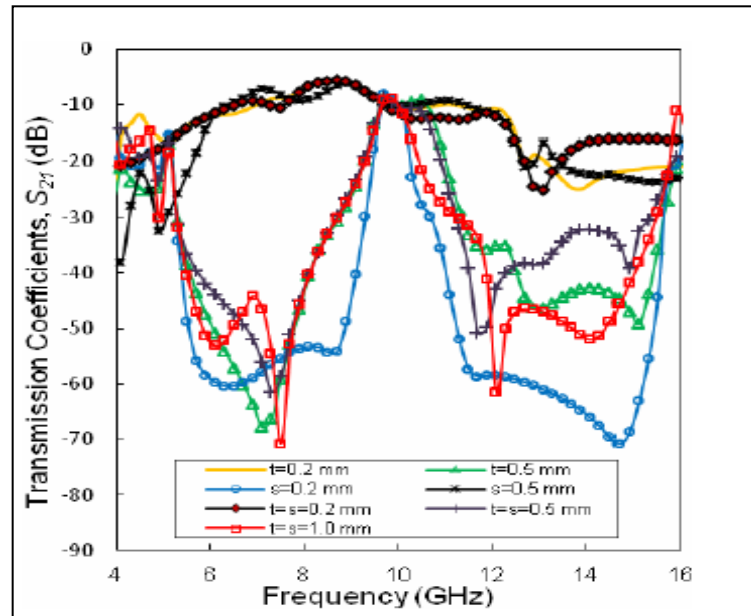


Figure 2.13: Transmission loss S_{21} of three by three EBG array with bridge width variation (Alam, Islam, & Misran, 2012).

2.5 Spiral EBG Structure Characteristics

A study was conducted by (Lin, Fang, & Zhang, 2008) focused on EBG characteristics enhancement by designing spiral structure. This study shows the unique behaviors of spiral design compared to a conventional EBG design. The turns of the spiral forms an L-C network due to the current flow on its metallic strips. Thus, this flow introduces an equivalent inductance L , where the gaps between the metallic sections introduce an equivalent capacitance C . As a result, a two-dimensional periodic L-C network is realized by a resonance frequency of the band-gap. The resonance can be determined by $\omega_0 = 1/LC$. Figure 2.14 (a) illustrates the conventional EBG and spiral EBG structures in an array of 5 by 3 each. Suspended Microstrip line method was used for both designs. The transmission coefficient S_{21} is shown in Figure 2.14 (b). The spiral design showed significant enhancement around 3 GHz and was very obvious from 5 to 8 GHz.

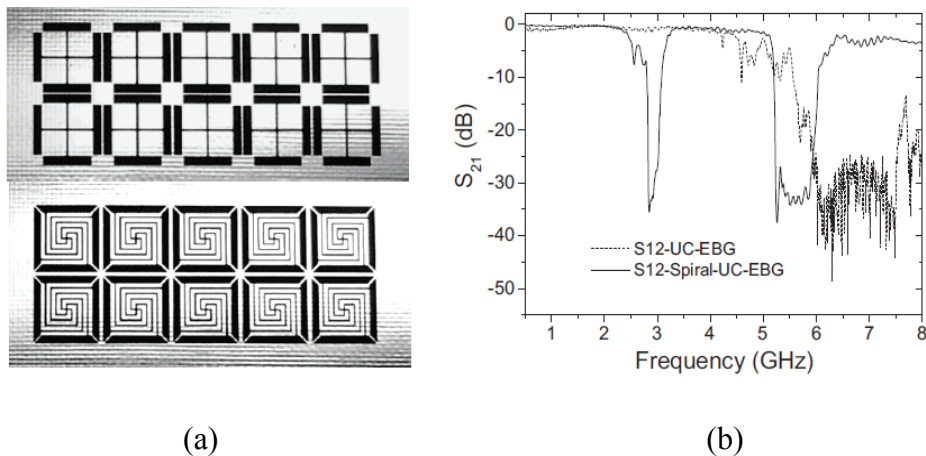


Figure 2.14: Transmission loss S_{21} of three by three EBG array with bridge width variation (Alam, Islam, & Misran, 2012).

The spiral EBG structure has a unique behavior that makes it possible to decrease the center frequency of the band-gap. The shape of the structure is formed by cutting slots

on a metallic patch. In other words, it is possible to have more compact EBG structures but with the cost of lower bandwidth. A study was conducted by (Moghadas et al., 2008) investigates the major parameter that can control the center frequency of the band-gap region which is the number of spiral turns in comparison to mushroom like EBG planar. The circular spiral EBG is shown in Figure 2.15 (a). The transmission coefficient of 3 by 3 planar is illustrated in Figure 2.15 (b).

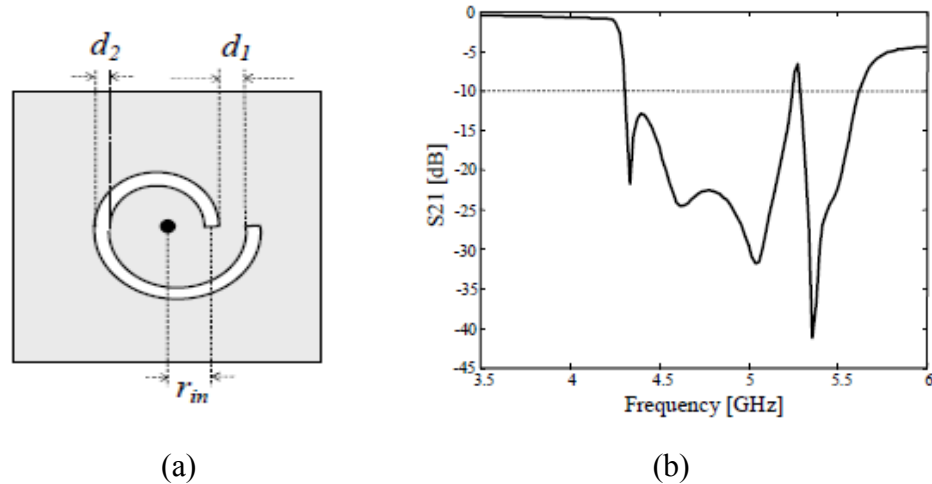


Figure 2.15: (a) Circular spiral EBG structure (b) Transmission coefficient S_{21} of circular EBG planar (Moghadas et al., 2008)

The effect of turns on the center frequency and fractional bandwidth of the structure is investigated as shown in Table 2.1. The increase of the number of spiral turns results in lower center frequency and reduction in the bandwidth.

Table 2.1: Turns effect on f_c and BW reduction (Moghadas et al., 2008)

SPIRAL TURNS (T)	f_c (GHZ)	BW (%)
1	3.32	22.40
1.25	2.86	20.00
1.5	2.44	16.80
1.7	2.11	13.70

$$(r_{in} = d_1 = d_2 = 0.2 \text{ mm})$$

As can be seen in Table 2.1, it is obvious that the center frequency of spiral structure has been reduced to 2.11 GHz and the related bandwidth to 13.70%.

2.6 An Overview of EBG Application for EMI Suppression on PCBs

Developing printed circuit boards that will pass legally required EMC tests is not difficult by incorporating design techniques for EMC compliance (Montrose, 2000). A PCB is a dielectric structure with both internal and external wiring that allows components and interconnects to be mechanically supported and electrically connected. Interconnects between layers are by vias. These vias can be plated and filled with metal to provide electrical connection between layers. Solid planar structures provide power and ground to components. Signal lines are distributed among various layers to provide interconnects.

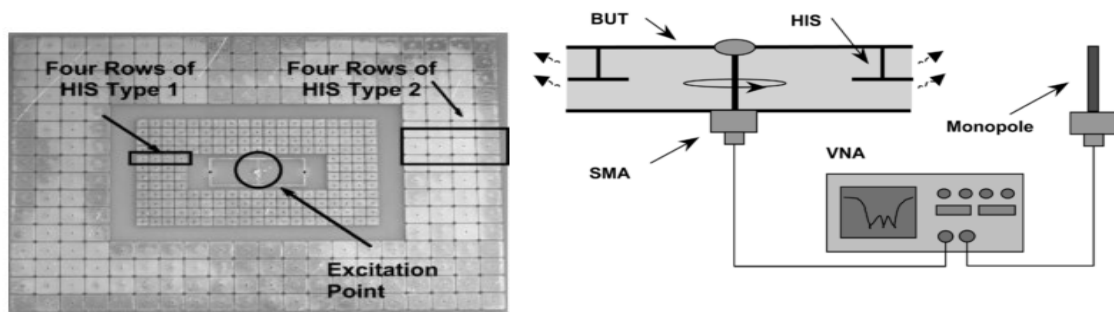
An important consideration in the design and specification of a PCB includes both the propagation delay of a transmitted signal and crosstalk between circuits, traces, and interconnects (Sunil. R. Gagare, 2014). Board material has become more than just physical support for conductors. Materials used form part of the circuit, dictating length, width, and spacing of traces. It is worth noting that for frequencies above 500 MHz, signal traces becomes part of the circuit that includes distributed resistance, capacitance, and inductance. At higher frequencies, the dimensions of the transmission line play a significant role in defining performance as the sources of noise are less numerous and relatively easy to be identified to prevent possible antenna parts from being driven relative to one another by these sources (Hubing, 2003). Changing any dimension can dramatically alter the board performance.

EBG materials have been widely considered in microwave circuits due to their unique electromagnetic properties for performance improving. The effectiveness of proposed EBGs through several PCBs by other researchers and its applications are discussed in the following subtopics.

2.6.1 EBG Structure for SSN Suppression

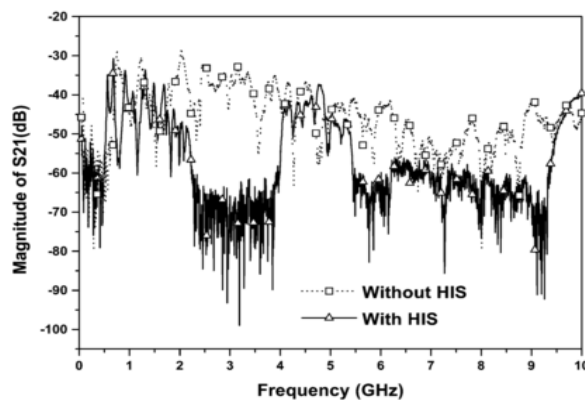
In high-speed digital circuits, the flow of the time-varying currents through vias between in multi-layer PCB design, result in radiations as well as switching noise (SSN) which is often induced in such circuitries. This noise is created whilst many outputs of a digital circuit switch at the same time. In addition, SSN depends on the geometry of the PCB. Therefore, it cannot be quantified precisely. Current traces are another issue where various studies have been concentrated on modeling this phenomenon (Shahparnia & Ramahi, 2007). The rapid increase of frequency clock is another primary source of switching noise.

Recently, the uses of electromagnetic bandgap (EBG) structures have been introduced as an inexpensive effective method for SSN suppression in the gigahertz frequency bands (Shahparnia et al., 2004). By introducing the EBG structure to PCB design, it is possible to suppress switching and other noise generated within boards for frequencies in the gigahertz frequency range. In the work of (Shahparnia et al., 2004), the EBG cells have been surrounding the port of excitation as shown in Figure 2.16 (a) . Later, the board was going under test by using a monopole antenna that will detect the radiated signals from the board as illustrated in Figure 2.16 (b). The results shows significant reduction of the incoming noise as shown in Figure 2.16 (c).



(a)

(b)



(c)

Figure 2.16: (a) HIS EBG structure cascading board (b) Experiment set up of RE test. (c) Transmission coefficient S_{21} comparison of PCB with and without EBG structure.

2.6.2 EBG Structures on Parallel-Plate

In a study conducted by (Abhari & Eleftheriades, 2003), an EBG structure was initially designed by utilizing an approximate circuit model and characterized by analytical solutions using the transverse resonance method, as well as full-wave finite-element simulations as shown in Figure 2.17 (a). The designed EBG surfaces were fabricated and employed in a number of parallel-plate waveguides (PPW) test board. As can be seen from Figure 2.17 (b), the transmission coefficient S_{21} shows a bandgap from 1.95 to 5.3 GHz. These results are significant although the EBG structure was not integrated into high-speed board with actual components.

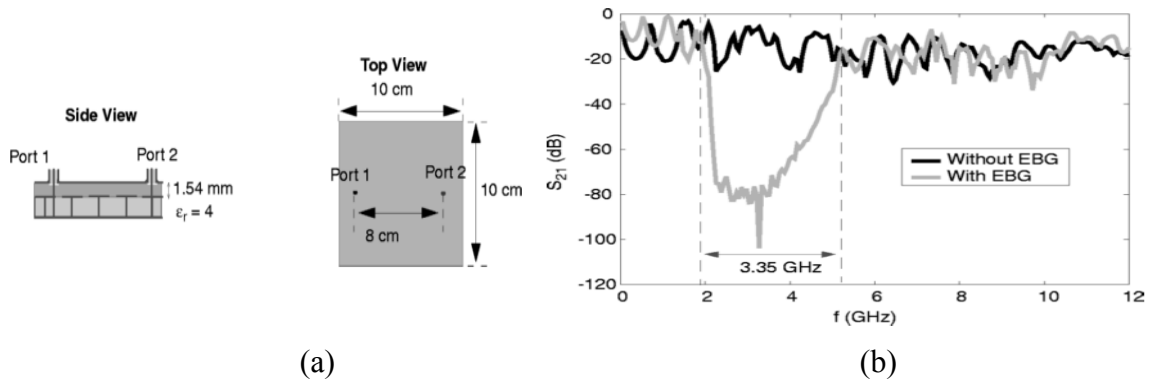


Figure 2.17: (a) EBG structure on parallel plate. (b) Transmission coefficient S_{21} comparison of parallel plate with and without EBG structure.

2.6.3 EBG Structure on Optical Transceiver

Another interesting method to suppress the noise level was introduced with the use of EBG structure and the shielding scheme as shown in Figure 2.18 (a) (Kawase et al., 2011). Figure 2.18 (b) shows the field potential ratio at an observation point. The horizontal axis is frequency and the vertical axis is a power ratio which is defined as voltage at the

observer position over the output voltage from the dipole. This result shows the energy component of 21 GHz to 24 GHz is decayed when transmitted to the observer. Therefore, the existence of the stop band is at this frequency range. As shown in Figure 2.18 (c), eight diaphragms were set up in the waveguide. The size of the diaphragm was determined to be $12 \text{ mm} \times 3.9 \text{ mm} \times 0.6 \text{ mm}$ with a spacing of 0.6 mm . A small dipole, as a noise source, is put into the wave guide on the left side 24.6 mm apart from the EBG. The depth of diaphragms was one-quarter wavelength of the target frequency of 20 GHz . When the frequency of the incident wave target is 20 GHz , the top surface becomes a high impedance surface, and the incident wave is reflected by mode mismatch in the waveguide.

The transmitted wave was measured at an observer position. Figure 2.18 (d) summarizes the peak emission values. Frequency ranges are per IEEE803.2ae and 10 GFC. This work has shown significant improvement as observed especially at 20.3125 GHz and 21.0375 GHz of horizontal polarization.

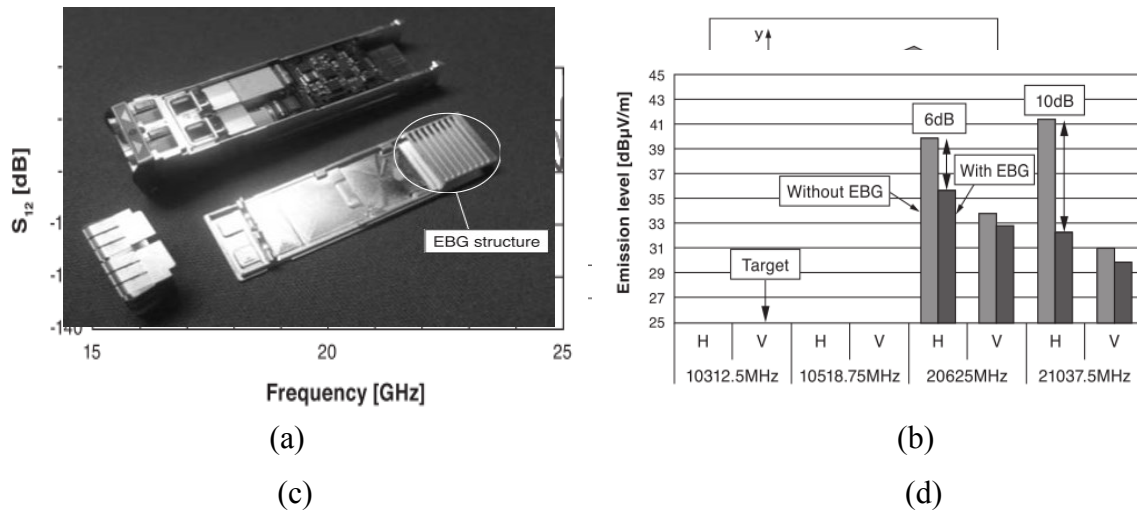


Figure 2.18: (a) Optical transceiver. (b) EBG structure and experimental set up. (c) Measured S_{21} at 5 cm distance by monopole antenna (d) RE test readings.

2.6.4 Split-Ring Resonators on High-Speed Circuits

The work conducted by (Bait-Suwailam & Ramahi, 2010) suggested a novel concept for mitigating switching noise propagation on high-speed printed circuit boards. through the introduction of etching complementary split-ring resonators (CSRRs) on only one metallic layer of the printed circuit board as shown in Figure 2.19 (a). This behavior is in contrast to the split-ring resonator that suppresses the magnetic field as this technique suppresses electrical field. Furthermore, by cascading CSRRs, concentrically, a wide suppression of switching noise covering a wide frequency band can be achieved. The drawback of this design was the need of cascading to obtain a bandgap at high frequency. As illustrated in Figure 2.19 (b), the CSRR structure has a stop band from 3 to 7 GHz and from 7 to 10 GHz.

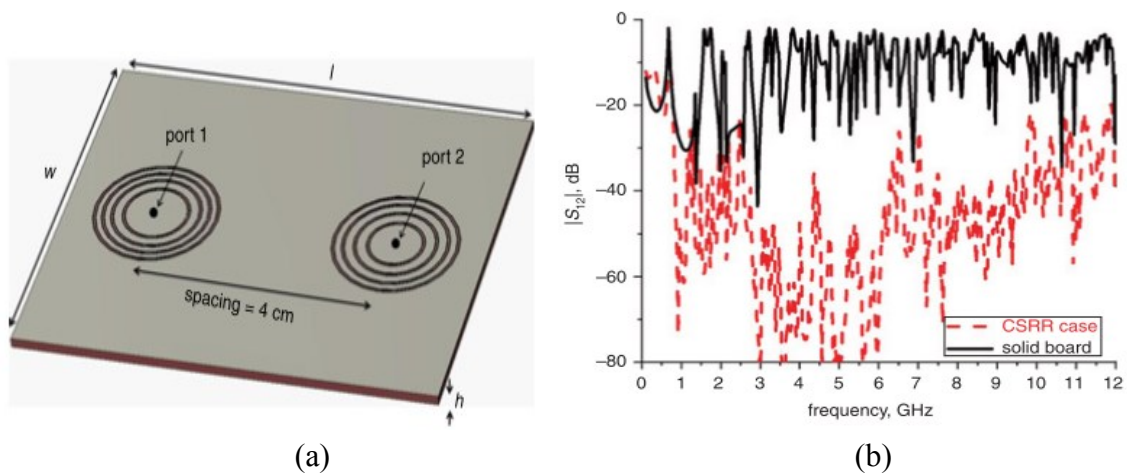


Figure 2.19: (a) Complementary split-ring resonator PCB. (b) Transmission coefficient S_{21} comparison of CSRR and solid board.

2.7 Summary

EBG structures with their modeling procedure, classifications and operation characteristics, including several applications of EBG applied for EMI reduction on PCBs have been presented and reviewed. Electromagnetic bandgap structures were reviewed with their capability of suppressing EMI on PCBs. The useful applications of deploying 2-D EBGs were addressed and their advantages and disadvantages were identified in terms the overall operation performances.

The existing researches have illustrated good agreement with the theoretical background of the EBG. In this work, spiral EBG structures will be designed and fabricated based on the lumped-element model. Spiral EBGs have the advantage of smaller size, lower cost, and wider bandwidth characteristics. The substrate material that will be used is FR4 due to its low cost and availability. The EBG structure will not involve vias to make the design easier to be integrated into PCBs as well as its fabrication.

The methods of dispersion diagram and suspended microstrip line will be used for the purpose of analysis the characteristics of proposed EBG design. On other hand, this work proposes a high-speed PCB that will be involved to ensure the existence of high radiated emissions by violating some of EMC guidance. These violations will increase the radiation level. In addition, the passive components will be used with the alert of their behavior at high frequency. Finally, the proposed EBG and high-speed PCB will be integrated for the purpose of EMI reduction.

- Alam, M. S., Islam, M. T., & Misran, N. (2012). A Novel Compact Split Ring Slotted Electromagnetic Bandgap Structure for Microstrip Patch Antenna Performance Enhancement. *Progress In Electromagnetics Research Research*, 130 (June), 389–409.
- Alshargabi, M. A., Abidin, Z. . Z., & Jenu, M. Z. M. (2015). High Speed PCB & Spiral with Patch EBG Planar Integration for EMI Reduction, *International Conference on Computer, Communication and Control Technology (I4CT)*, 584–588.
- Aminian, A., Yang, F., & Rahmat-Samii, Y. (2003). In-phase reflection and EM wave suppression characteristics of electromagnetic band gap ground planes. *IEEE Antennas and Propagation Society International Symposium*,(4), 430–433.
- Fei, H., Guo, H., Liu, X., & Wang, Y. (2011). A Novel Compact EBG Structure for Mutual Coupling Reduction in a Patch Array. *Progress In Electromagnetic Research Symposium*, (1), 12–15.
- Gagare, S. R., & Kachare, A. E. (2014). EMI/EMC Analysis and Noise Reduction in High Frequency Devices. *International Journal Of Engineering Sciences & Research Technology*, 3(7), 6.
- I., M. (2000). Printed Circuit Board Design Techniques for EMC Compliance: A Handbook for Designers.
- Inder Bahl. (2003). Lumped Element for RF and Microwave Circuits. ARTECH HOUSE.
- Islam, M. T., & Alam, M. S. (2013). Compact EBG Structure for Alleviating Mutual Coupling Between Patch Antenna Array Elements. *Progress In Electromagnetic Research*, 137.
- Kawase, D., Oomori, H., Kawamura, H., Kondou, T., Shiozaki, M., & Kurashima, H. (2011). EMI suppression of 10 Gbit/s optical transceiver by using EBG structure. *SEI Technical Review*, (73), 98–103.
- Kim, C.-S. K. C.-S., Park, J.-S. P. J.-S., Ahn, D. A. D., & Lim, J.-B. L. J.-B. (2000). A novel 1-D periodic defected ground structure for planar circuits. *IEEE Microwave and Guided Wave Letters*, 10(4), 131–133.
- Lin, B. Q., Fang, L., & Zhang, H. M. (2008). A novel planar spiral EBG structure with improved compact characteristics. *Proceedings of 2008 Asia Pacific Microwave Conference, APMC 2008*, 8–11.
- Moghadasi, S. M., Attari, A. R., & Mirsalehi, M. M. (2008). Comparison between Various Compact Electromagnetic Band-gap (EBG) Structures for Coupling Reduction in Antenna Arrays, *Progress In Electromagnetics Research* (1), 175–178.

- Mohajer-iravani, B., Shahparnia, S., Ramahi, O. M., & Member, S. (2014). Electromagnetic Band Gap Structures in MSA. *International Journal of Computer Applications*, 48(2), 292–303.
- Ouassal, H., Shaker, J., Roy, L., & Chaharmir, R. (2016). A novel multi-layer electromagnetic band gap structure (EBG) comprised of 3-D lattice of square rings. *IEEE MTT-S International Conference on Numerical Electromagnetic and Multiphysics Modeling and Optimization, NEMO 2015*, (1), 3–6.
- Phuong, H. N. B., Chien, D. N., & Tuan, T. M. (2013). Novel Design of Electromagnetic Bandgap Using Fractal Geometry. *International Journal of Antennas and Propagation*, 2013(1), 1–8.
- Sievenpiper, D., Zhang, L., Broas, R. F. J., & Yablonovitch, E. (1999). High-impedance electromagnetic surfaces with a forbidden frequency band. *IEEE Transactions On Microwave Theory And Techniques*. 47(11), 2059–2074.
- Yang F. and Rahmat-samii Y., (2003), Electromagnetic Band Gap Structure in Antenna Engineering.
- Yang F., and Rahmat-samii Y. (2003), Reflection Phase Characterizations of the EBG Ground Plane for Low Profile Wire. *IEEE Transactions on Antennas and Propagation*, 51(10), 2691–2703.

APPENDIX A

MATHEMATICAL CALCULATIONS